Computers & Operations Research 170 (2024) 106765

Contents lists available at ScienceDirect

Computers and Operations Research

journal homepage: www.elsevier.com/locate/cor

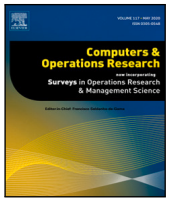

Unmanned aerial vehicle variable radius set covering problem for emergency wireless network

Youngsoo Park [a], Chang Seong Ko [b], Ilkyeong Moon [c,d,*]

[a] Woowa Brothers Corporation, Seoul 05544, Republic of Korea
[b] Department of Industrial and Management Engineering, Kyungsung University, Busan 48434, Republic of Korea
[c] Department of Industrial Engineering, Seoul National University, Seoul 08826, Republic of Korea
[d] Institute of Engineering Research, Seoul National University, Seoul 08826, Republic of Korea

ARTICLE INFO

Keywords:
OR in disaster relief
Branch-and-price
Column generation
Set covering problem
Unmanned aerial vehicle

ABSTRACT

The utilization of unmanned aerial vehicles (UAVs) has garnered increasing interest across various disciplines. The idea of smart cities led to the exploration of using UAVs in the public service industry, with a focus on integrating all aspects of the system through information and physical items. In this paper, we introduce and model the operational problem of using UAVs to construct an emergency wireless network in a disaster situation using the set covering approach. Unique to our study is the consideration that UAVs do not require predetermined positioning or altitude specifications. Consequently, the problem described in this paper can be classified as a *planar variable radius covering problem*, which involves a nonconvex continuous relaxation feasible set. We introduce the application of the Dantzig–Wolfe decomposition alongside a branch-and-price algorithm to tackle this problem. Additionally, the pricing subproblem's solvable equivalent formulation is ingeniously derived from existing theories on the minimum covering circle. For large-scale instances, we propose a heuristic derived from an extended formulation. Comparative computational experiments demonstrate that our proposed algorithms significantly surpass the efficiency of the benchmark genetic algorithm previously reported in the literature.

1. Introduction

Unmanned aerial vehicles (UAVs) can reach a target in a three-dimensional trajectory, allowing rapid access to remote areas and heavily congested city centers. Moreover, *autonomous* flight without human intervention is allowed nowadays, owing to advanced positioning and controlling technologies. The emergence of smart city concepts has further catalyzed the exploration of UAVs as versatile tools, offering quick and adaptable solutions not only in commerce but also in social services. UAVs serve as pivotal links, bridging the gap between disparate urban elements and central authorities. The inspection and maintenance of infrastructure, the monitoring of traffic conditions, the monitoring of vulnerable security points, and the identification of and response to disasters are all areas that have been investigating UAV possibilities.

The utility of UAVs becomes particularly evident in unforeseen circumstances. Their ability to navigate without disrupting ground traffic and to adapt to rapidly changing environments is driving an immense interest in utilizing UAVs in disaster management. Van Wassenhove (2006) delineates disaster management into four phases: *mitigation*, *preparedness*, *response*, and *rehabilitation*. In the response phase, starting right after the disaster, humanitarian logistics mobilizes not only human and material resources but also skills and information between authorities and the disaster areas (Van Wassenhove, 2006). In such scenarios, timely information about the disaster site and survivors is critical for devising effective rescue strategies. There have been numerous instances where disaster victims have utilized social media platforms like X (Twitter) and Facebook for disseminating vital information regarding their situation and aid efforts (Wallop, 2011).

In environments ravaged by disaster, where the network infrastructure is incapacitated due to extensive disruptions, there have been attempts to recover temporary wireless network connections by UAV-mounted wireless routers/access points. The literature reveals a rich investigation into routing- and covering-based methodologies for UAV system deployment (Park et al., 2020). Routing-based strategies enable UAVs to traverse through multiple waypoints, facilitating data collection from sensors or conducting area surveillance with UAV-mounted cameras. Conversely, the covering-based approach positions UAVs with integrated wireless routers to hover over specific areas,

* Corresponding author at: Department of Industrial Engineering, Seoul National University, Seoul 08826, Republic of Korea.
E-mail addresses: simulacrum@snu.ac.kr (Y. Park), csko@ks.ac.kr (C.S. Ko), ikmoon@snu.ac.kr (I. Moon).

https://doi.org/10.1016/j.cor.2024.106765
Received 6 June 2023; Received in revised form 8 June 2024; Accepted 1 July 2024
Available online 6 July 2024

thereby maintaining temporary network connectivity. A pivotal advantage in deploying UAVs, underscored in both methodologies, is their operational flexibility. Unlike with classical vehicle routing and discrete facility location problems, UAV flight positions are not constrained to predetermined locations in such a setup.

Berman et al. (2009) introduced the variable radius covering problem, exploring both *planar* and *discrete* scenarios, thereby augmenting classical covering-based facility location problems by allowing the facility's coverage radius to be a variable in the decision-making process. This research embraces the *planar variable radius covering problem* (VCP) framework proposed by Berman et al. (2009) for modeling the UAV-based wireless network location problem. In VCP, facilities (UAVs) can be freely positioned on the Euclidean xy-plane, unrestricted by predefined locations. A facility is deemed to *cover* a demand point if the distance to the point is within its coverage radius, with the coverage potential being binarized based on this distance and radius. The VCP's goal is to minimize costs associated with facility operation and its coverage radius.

Although Berman et al. (2009) predates the widespread adoption of UAV technology, its principles align closely with the operational challenges of UAV deployment. UAVs, in this context, offer flexible location choices akin to those in continuous facility location problems, and can adjust their coverage radius by altering flight altitudes, thereby directly correlating operational costs with coverage scope. Park et al. (2020) applied the set covering approach to the UAV-based network location problem, considering the planar aspect of facility location to fully leverage UAV capabilities. Notable technological and methodological gaps remain, necessitating further research. Berman et al. (2009) developed a mathematical framework for the VCP, yet it lacked a solvable representation for optimization solvers, leading to a reliance on heuristic and metaheuristic approaches. Conversely, Park et al. (2020) formulated the UAV set covering problem (USCP) and devised a branch-and-price-based exact algorithm, but it presupposed a fixed-radius coverage, thereby constraining UAV flight altitude to a singular level. This assumption simplifies the complex dynamics of UAV operation, where, as Berman et al. (2009) noted, the coverage radius should flexibly adjust according to the UAV's capabilities and operational altitude.

This research advances the discourse by proposing a model that allows for continuous determination of the coverage radius, thereby reflecting the nuanced decisions related to UAV altitude. Such an approach not only enhances the solutions proposed by previous studies but also broadens the spectrum of practical applications, enabling more effective UAV operations across varied altitudes and coverage distances. Moreover, the operational costs associated with UAV deployment are modeled as a monotonically increasing function of coverage size, acknowledging the decreased propeller efficiency and increased energy demands at higher altitudes due to lower air density (Liu et al., 2019; Paredes et al., 2017). This cost structure aligns with the pragmatic challenges of UAV operations, as is also supported by Berman et al. (2009).

Herein, we revisit the planar VCP as introduced by Berman et al. (2009), enhancing it with the UAV-specific considerations of the USCP (Park et al., 2020). This study is hence articulated around the UAV variable radius set covering Problem (UVCP), modeled as a mixed-integer quadratically constrained quadratic program. Employing the Dantzig–Wolfe decomposition, we reformulate the UVCP into an extended formulation that efficiently solves the exact problem through a branch-and-price algorithm. This methodology leverages the "minimal subset" concept proposed by Berman et al. (2009), circumventing the exhaustive brute force subset evaluation with a column generation strategy.

Nonetheless, the adaptation of techniques of Park et al. (2020) to the UVCP, characterized by its continuous coverage radius decision variable, presented challenges because of the nonconvex nature of the problem's feasible set. To address this, we introduce a solvable equivalent subproblem employing linear constraints and minimal covering circle principles. Given the complexity of solving large-sized instances, a heuristic that discretizes and fixes the coverage radius, aligning with the USCP framework, is proposed. Computational experiments demonstrate the superior performance of our algorithms compared to the genetic algorithm approach of Berman et al. (2009). Note that this study focuses on addressing the facility location problem in a broad manner by linking the characteristics of UAVs, rather than by dealing with the actual physical variable coverage of UAV-based wireless networks.

The structure of the remainder of this paper is as follows: Section 2 summarizes the literature related to the research. Section 3 defines the UVCP and outlines the mathematical model. Section 4 details the reformulation of the UVCP and the branch-and-price algorithm. Section 5 introduces the solvable equivalent subproblem and its underlying rationale. The heuristic for fixed coverage radius is presented in Section 6, followed by a comparison of algorithmic performances in Section 7. Finally, Section 8 summarizes the findings and contributions of this research.

2. Literature review

Distinctive features set the work of Berman et al. (2009) and Park et al. (2020) apart from existing literature. Primarily, the decision regarding the UAVs' locations is continuous, diverging from traditional continuous facility location problems that presuppose a fixed number of facilities (Comley, 1995; Drezner et al., 2001; Plastria, 2001; Capoyleas et al., 1991; Periyasamy et al., 2016). Addressing the optimal number of UAVs as a variable introduces complexities beyond the scope of existing continuous facility location methodologies. Also, although discrete facility location problems through set covering (Daskin, 1983; Gendreau et al., 1997; Zorbas et al., 2016; ReVelle and Hogan, 1989) and median-based approaches (Choi and Chaudhry, 1993; Daskin and Maass, 2015; Wankmüller et al., 2020) consider the number of facilities as a variable, they restrict UAV locations to predefined points, thus not fully exploiting UAV flexibility. Recent literature, including (Karatas and Eriskin, 2021, 2023) and notably (Blanco et al., 2023), has explored the interplay between discrete and continuous decision-making in facility location problems, with a focus on optimizing location and coverage radius simultaneously. However, this research distinguishes itself by addressing the minimum covering problem with continuous, facility-independent coverage radii, diverging from the maximal covering location models and facility-dependent radii approaches prevalent in existing studies. A comparative analysis of this research with existing studies is detailed in Table 1. For a comprehensive literature review on covering-based facility location problems, readers are directed to Farahani et al. (2012), and for health care–specific location problems, readers are directed to Bélanger et al. (2019) and Ahmadi-Javid et al. (2017).

As mentioned in Section 1, the UVCP assumes the coverage radius-related objective function. Berman et al. (2009) defines the coverage cost function according to the classical research of Drezner (1998) and Fernández et al. (2007). For the land-based infrastructure, the coverage distance is directly related to the cost assumption, where the variable cost is non-decreasing in the coverage radius. As an example, Drezner (1998) suggested four variable costs, $\phi(r)$, as functions of the coverage radius r: $\phi(r) = Cr^2$, $\phi(r) = Cr(1 + \alpha r)$, $\phi(r) = Cr$, and $\phi(r) = C\sqrt{r}$.

On the other hand, when the UAV is used as an airborne device, the operational cost should be defined based on practical models. A vast amount of literature has studied the energy assumption of UAVs under various missions. There is research focused on optimizing the transmitting power of UAV-based wireless networks. Wang et al. (2020) provided an energy-efficient deployment algorithm for a UAV-based wireless platform, claiming that the optimal operating altitude is

Table 1
Comparison of this research and existing literature.

Author (year)	Type	Given candidate positions	Fixed numberof facilities
Comley (1995)	Continuous	No	Yes
Drezner et al. (2001)	Continuous	No	Yes
Plastria (2001)	Continuous	No	Yes
Capoyleas et al. (1991)	Continuous	No	Yes
Periyasamy et al. (2016)	Continuous	No	Yes
Blanco et al. (2023)	Continuous	No	Yes
Daskin (1983)	Set cover	Yes	No
Gendreau et al. (1997)	Set cover	Yes	No
Zorbas et al. (2016)	Set cover	Yes	No
ReVelle and Hogan (1989)	Set cover	Yes	Yes
Karatas and Eriskin (2021)	Set cover	Yes	No
Choi and Chaudhry (1993)	Median	Yes	Yes
Daskin and Maass (2015)	Median	No	Yes
Wankmüller et al. (2020)	Median	Yes	No
Karatas and Eriskin (2023)	Median	Yes	No
Berman et al. (2009)	Set cover	No	No
Park et al. (2020)	Set cover	No	No
This research	Set cover	No	No

linearly proportional to the target coverage distance. Both Wang et al. (2020) and Sun et al. (2019) modeled convex altitude-radius curves but considered wireless transmitting power as the operational cost. The primary driver of energy consumption is propulsion, which can be used to model the operational cost of UAV deployment. This cost can be modeled as a monotonically increasing function of coverage size, acknowledging the decreased propeller efficiency and increased energy demands at higher altitudes due to lower air density (Liu et al., 2019; Paredes et al., 2017). Thibbotuwawa et al. (2019) modeled the power consumption of a UAV as $p = \frac{T^{3/2}}{\sqrt{2D\varsigma}}$, where T is a given thrust, ς is a facing area of the UAV, and D is the air density. Because the air density is inversely proportional to the altitude H, the power consumption of UAV can be modeled as $p \propto \sqrt{H}$. Abeywickrama et al. (2018) measured the energy consumption of basic maneuvering operations of UAVs through empirical experiments. The energy consumption followed a linear function of the hovering altitude, expressed as $p \propto H$.

As mentioned in Sun et al. (2019), the UAV altitude versus coverage radius cannot be explicitly written as a function of each other. Instead, one can approximate the relationship between the coverage radius and flight altitude as a quadratic function based on the convex and symmetric curves shown in Wang et al. (2020) and Sun et al. (2019). Under that assumption, the power consumption of UAVs can be represented as a function of the coverage radius. According to the models by Thibbotuwawa et al. (2019) and Abeywickrama et al. (2018), the power consumption of UAVs can be modeled as $p = Cr$ and $p = Cr^2$, respectively.

3. Problem description

This section delineates the UAV variable radius set covering Problem (UVCP), building upon the framework established by Park et al. (2020), where UAVs are deployed to form wireless networks covering designated demand points. The set covering model is employed, prioritizing coverage over considerations such as battery constraints or specific flight paths to each location, due to the model's simplification intent. This problem formulation is particularly tailored for emergency response planning in disaster scenarios, demanding a robust solution capable of accommodating all potential demands. While the primary aim is to minimize resource usage, the focus diverges from profit maximization to ensure maximum operational responsiveness in the face of rapidly evolving disaster contexts. The UVCP adapts the assumptions from the UAV set covering problem (USCP) as defined by Park et al. (2020), with a singular, yet significant modification:

1. The information on the positions of demand points is already known.
2. UAVs are unrestricted in their hovering positions within the xy-plane.
3. A demand point is considered covered if it falls within a UAV's coverage circle.
4. The wireless network faces no transmission capacity constraints.
5. UAV operations are not impeded by overlap interference or shadowing effects from structures.
6. UAVs in the UVCP exhibit variable coverage distances.

The distinction lies in the last assumption, introducing variable UAV flight altitudes to enable diverse wireless network coverage distances. While not explicitly limiting the coverage distance range, incorporating such constraints into the solution algorithm remains straightforward. Previous work by Berman et al. (2009) omitted explicit coverage radius limitations, a choice driven by heuristic and metaheuristic implementation challenges. For a comparative analysis of algorithmic performance within this study, these upper or lower limits of coverage distance constraints are similarly bypassed, though their inclusion would not complicate the algorithmic structure and could potentially enhance computational efficiency because of the smaller solution space.

Consistent with Park et al. (2020), demand point data is treated as initial, amendable input, reflecting operational flexibility. UAV resource consumption is quantified through the aggregation of fixed costs and variable costs associated with coverage radius. Minimizing the number of operational UAVs, as well as their flight altitudes and respective coverage radii, is crucial for preserving UAV flight capabilities and optimizing resource deployment.

An illustrative overview of the UVCP is provided (refer to Fig. 1), showcasing the free positioning of UAVs within the xy-plane and the unbounded determination of network coverage radii. This visual representation emphasizes the strategic deployment of UAVs to form optimally tight coverage circles around assigned demand points, underscoring the concept of minimal subsets introduced subsequently.

3.1. Mathematical model

Berman et al. (2009) proposed a mathematical model of the UVCP and named it as the planar variable radius covering problem. For the unity of the research, the notations are modified as follows:

Set

N set of demand points.

Parameters

$a_i^{\hat{x}}$ position of demand point i on x-coordinate. $\forall i \in N$

$a_i^{\hat{y}}$ position of demand point i on y-coordinate. $\forall i \in N$

F fixed cost of operating one UAV.

Decision variables

$$y_j = \begin{cases} 1, & \text{if UAV } j \text{ is operated.} \\ 0, & \text{otherwise.} \end{cases} \quad \forall j \in \{1, ..., |N|\}$$

$c_j^{\hat{x}} \in \mathbb{R}$, position of UAV j on x-coordinate. $\forall j \in \{1, ..., |N|\}$

$c_j^{\hat{y}} \in \mathbb{R}$, position of UAV j on y-coordinate. $\forall j \in \{1, ..., |N|\}$

$r_j \in \mathbb{R}$, coverage radius of UAV j. $\forall j \in \{1, ..., |N|\}$

$$x_{ij} = \begin{cases} 1, & \text{if demand point } i \text{ is allocated to UAV } j. \\ 0, & \text{otherwise.} \end{cases} \quad \forall i \in N, \ \forall j \in \{1, ..., |N|\}$$

A noteworthy deviation from the original model posited by Berman et al. (2009) is the treatment of the decision variable y_j regarding the operation of facilities, or in the context of this research, UAVs. Instead, they claimed that the operational count of facilities, represented as p, with each facility indexed within the set $1, \ldots, p$, should be determined as part of the solution. This model, however, presented challenges for direct application in mathematical programming solvers because of the self-referential nature of the decision variable and its indices.

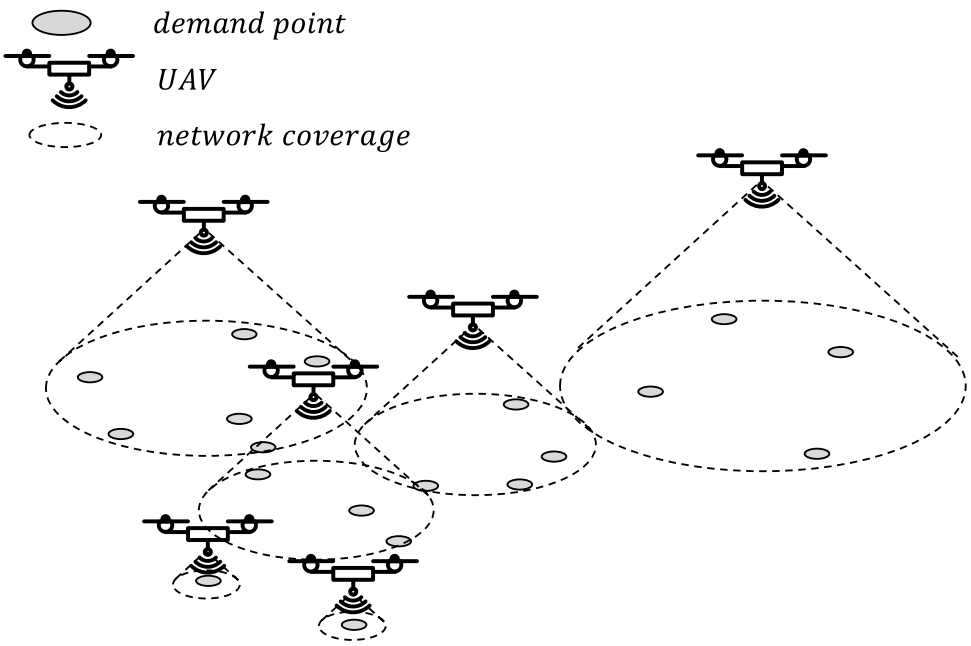

Fig. 1. Overview of the UVCP.

Recognizing that the number of UAVs required for covering problems does not surpass the total number of demand points, denoted as $|N|$, our approach introduces a binary decision variable y_j. This variable indicates whether UAV j is operational, utilizing the comprehensive set $1,\dots,|N|$ for indexing. Further drawing on the work of Berman et al. (2009), the Euclidean distance from demand point i to UAV j is denoted as $d_i\left((c_j^{\hat{x}}, c_j^{\hat{y}})\right)$, with the operation cost associated with UAV coverage radius r represented by $\phi(r)$. Adhering to the cost structure advocated by Drezner (1998) and Fernández et al. (2007), a quadratic relationship between coverage radius and cost, $\phi(r) = r^2$, is adopted for its simplicity and relevance. The foundational model proposed by Berman et al. (2009) is articulated as follows:

[Original formulation of Berman et al. (2009)**]**

$$\min \quad pF + \sum_{j=1}^{p} \phi\left(\max_{i\in N}\left\{ x_{ij} d_i\left((c_j^{\hat{x}}, c_j^{\hat{y}})\right)\right\}\right), \tag{1}$$

$$\text{s.t.} \quad \sum_{j=1}^{p} x_{ij} \geq 1, \qquad \forall i \in N \tag{2}$$

$$x_{ij} \in \mathbb{B}, \qquad \forall i \in N, j \in \{1,\dots,p\} \tag{3}$$

Berman et al. (2009) claimed that the UVCP is not suitable for a mathematical optimization approach because of the self-dependence of the index and the inexplicit expression of the coverage radius, $d_i\left((c_j^{\hat{x}}, c_j^{\hat{y}})\right)$. However, based on the approaches proposed in Park et al. (2020), we formulate the UVCP as a mixed-integer quadratically constrained quadratic programming problem, paving the way for explicit mathematical modeling.

[Explicit Reformulation of the UVCP]

$$\min \quad \sum_{j=1}^{|N|} y_j F + \sum_{j=1}^{|N|} \phi(r_j), \tag{1'}$$

$$\text{s.t.} \quad x_{ij} \leq y_j, \qquad \forall i \in N, \forall j \in \{1,\dots,|N|\} \tag{4}$$

$$\sum_{j=1}^{|N|} x_{ij} \geq 1, \qquad \forall i \in N \tag{2'}$$

$$(a_i^{\hat{x}} - c_j^{\hat{x}})^2 + (a_i^{\hat{y}} - c_j^{\hat{y}})^2 \leq r_j^2 + \tilde{M}(1 - x_{ij}), \qquad \forall i \in N, \forall j \in \{1,\dots,|N|\} \tag{5}$$

$$x_{ij} \in \mathbb{B}, \qquad \forall i \in N, \forall j \in \{1,\dots,|N|\} \tag{3'}$$

$$y_j \in \mathbb{B}, \qquad \forall j \in \{1,\dots,|N|\} \tag{6}$$

$$c_j^{\hat{x}}, c_j^{\hat{y}}, r_j \in \mathbb{R} \qquad \forall j \in \{1,\dots,|N|\} \tag{7}$$

The reformulated UVCP bears resemblance to the Euclidean standard (ES) formulation of the USCP (Park et al., 2020), with two notable distinctions: the quadratic nature of the objective function, $\phi(r) = r^2$, reflecting variable operation costs as modeled in Berman et al. (2009) and Abeywickrama et al. (2018), and the treatment of coverage distance as a continuous decision variable rather than a fixed parameter. Despite achieving an explicit formulation, the inclusion of Constraint (5) results in a nonconvex continuous relaxation of the problem, rendering traditional commercial solvers, which rely on linear programming (LP) relaxation-based branch-and-cut algorithms, ineffective. Note that the solution algorithm designed for the UVCP can be used for quadratic and general convex objective functions.

Furthermore, in the USCP, the ES formulation could not even solve the smallest instances within an applicable computation time because of the weak continuous relaxation bounds and the symmetries of the problem. Considering that the UVCP has an extra decision on the coverage radius, r, it would be challenging to solve the explicit reformulation in its current form. To solve the problem, first, we decomposed the explicit reformulation of the UVCP to the extended formulation. As in the USCP, we used the fact that it is easy to find the optimal position and the size of the minimum covering circle if the set of demand points is given. By using similar generating sets as in the USCP, the UVCP is decomposed based on the decision variable x_{ij}. In the explicit reformulation of the UVCP, it is only necessary to show that Constraint (5) can be formulated linearly. In Section 5, the pricing subproblem II consists of mixed-integer linear constraints and has a polyhedral feasible set. Section 5.2 proves that two pricing subproblems are equivalent so that the UVCP can be solved by the branch-and-price (B&P) algorithm.

4. Branch-and-price approach to the UVCP

We reformulate the problem using a set-partitioning extended formulation, applying the Dantzig–Wolfe decomposition to encapsulate

column-wise decisions regarding the coverage of demand points by individual UAVs. This approach is predicated on the premise that a specific ensemble of demand points provides a unique minimum covering circle—termed a minimal subset. Berman et al. (2009) characterizes these subsets by a set of variables: x_{ij} representing the allocation decisions; r_j, the corresponding coverage radius; and $(c_j^{\hat{x}}, c^{\hat{y}}j)$, the UAV positioning coordinates. The comprehensive description of each minimal subset emerges from the allocation pattern of demand points, succinctly captured by xij. Berman et al. (2009) further elucidates that the optimal resolution of the UVCP encompasses a conglomeration of these minimal subsets. Utilizing the Dantzig–Wolfe decomposition, we can identify that the delineation of demand points within these subsets translates into columns forming part of an extended formulation. Upon selecting a particular set of demand points, we establish a unique minimum covering circle, with the coverage radius r_j equivalently mirroring the circle's radius. Consequently, the cost attributed to each column, denoted as g_k, amalgamates the fixed UAV cost F and the variable operational cost $\phi(r_k)$, reflective of the coverage radius. The collection of all feasible columns, signified by Ω, encapsulates every potential UAV coverage configuration over the set of demand points, with the binary decision variable z_k indicating the employment of column k, and the binary parameter w_{ik} specifying the assignment of demand point i to column k. The extended formulation of the UVCP is defined as follows:

[Extended formulation]

$$\min \quad \sum_{k\in\Omega} g_k z_k, \tag{8}$$

$$\text{s.t.} \quad \sum_{k\in\Omega} w_{ik} z_k \geq 1 \qquad \forall i \in N \tag{9}$$

$$z_k \in \mathbb{B} \qquad \forall k \in \Omega \tag{10}$$

The extended formulation of the UVCP aligns with the constraints observed in the USCP, albeit with a nuanced objective function (8) aimed at minimizing the aggregate resources requisite for comprehensive demand point coverage. Constraint (9) mandates coverage for each demand point, ensuring no point remains uncovered. Despite (Berman et al., 2009) providing a theoretical upper bound on minimal subsets $(|N|(|N|^2+5)/6)$, the practical challenge lies in discerning these subsets without resorting to an exhaustive brute-force search—owing to the exponential nature of possible subsets $(2^{|N|}-1)$. The column generation (CG) algorithm emerges as a pivotal mechanism in this context, dynamically generating columns that enhance the solution set from an extant column base. This pricing subproblem, focused on minimal subsets, is poised to yield a minimal number of columns essential for articulating the UVCP's solution landscape comprehensively. Within the CG framework, the restricted master problem (RMP) undergoes LP relaxation, with dual prices, π_i derived from Constraint (9). Solving the pricing subproblem facilitates the identification of demand point sets with minimal reduced costs, thereby introducing new columns into Ω should the objective value manifest a negative reduced cost. Uniquely, the pricing subproblem I diverges from its Euclidean branch-and-price algorithm (EBP) counterpart in Park et al. (2020), notably in its consideration of a variable coverage radius, r.

[Pricing subproblem I]

$$\min \quad F + \phi(r) - \sum_{i\in N} \pi_i x_i \tag{11}$$

$$\text{s.t.} \quad (a_i^{\hat{x}} - c^{\hat{x}})^2 + (a_i^{\hat{y}} - c^{\hat{y}})^2 \leq r^2 + \tilde{M}(1-x_i), \qquad \forall i \in N \tag{12}$$

$$x_i \in \mathbb{B}, \qquad \forall i \in N \tag{13}$$

$$r \in \mathbb{R}, \tag{14}$$

$$c^{\hat{x}}, c^{\hat{y}} \in \mathbb{R} \tag{15}$$

The first pricing subproblem I arises as a minimization problem, where the dual variable π_i stays nonnegative, ensuring that each solution outlines a circle enclosing all relevant demand points, thus creating a minimal subset. The subproblem I has an intuitive structure. Particularly, it is known that in the case of the fixed radius – the USCP – the subproblem is solved efficiently by the commercial solver. However, as mentioned in Section 3.1, the continuous relaxation of the feasible set is nonconvex because of Constraint (12). Therefore, the optimization solver cannot find the optimal solution of the pricing subproblem I. To circumvent these challenges, we propose an equivalent pricing subproblem, drawing from the principles of Heron's formula and the geometry of minimum covering circles.

5. Minimum covering circle-based approach

5.1. Formulation of the pricing subproblem II

The coverage constraint of the pricing subproblem I is modeled in a mixed-integer quadratic formulation. Constraint (12) relates a circle and a demand point by the distance between the center of the circle and the demand point and the radius of the circle. However, a circle can also be defined by two or three points. A minimum covering circle of two points is a circle whose diameter is the line connecting two points. When covering three points, if three points form an obtuse triangle, two points on the obtuse angle can define a minimum covering circle. If three points form a right or an acute triangle, a circumcircle defined by three points is a minimum covering circle. When a set of demand points is fixed, it is obvious that a minimum covering circle of the set has the largest radius among the minimum covering circles of its subsets. Thus, the constraint is valid for every two-element and three-element subset. On the other hand, because there exists a two-element or three-element subset that defines the minimum covering circle, by modeling the constraint for every two-element and three-element subset, the coverage distance constraint can be defined.

To model the minimum covering circle-based formulation, we define a parameter $d_{ab} := \|a-b\|_2$ as a distance between two demand points. Also, the distance between a demand point i and the UAV j, d_{ij}, can be defined as a decision variable instead of as the distance function, $d_i\big((c_j^{\hat{x}}, c_j^{\hat{y}})\big)$, used in Berman et al. (2009). However, if a position of a UAV j, $(c_j^{\hat{x}}, c_j^{\hat{y}})$, is given, d_{ij} can be calculated as being in between two demand points. For demand points a, b, and c, without loss of generality, let $d_{ab} \geq d_{bc}$ and $d_{ab} \geq d_{ca}$. Based on the formula for the circumradius of a triangle and Heron's formula, a radius of the covering circle, R_{abc}, is defined as:

$$R_{abc} := \begin{cases} d_{ab}/2, & \text{if } d_{bc}^2 + d_{ca}^2 \leq d_{ab}^2 \\ \dfrac{d_{ab}d_{bc}d_{ca}}{4\sqrt{S_{abc}(S_{abc}-d_{ca})(S_{abc}-d_{bc})(S_{abc}-d_{ab})}}, & \text{otherwise,} \end{cases}$$

where $S_{abc} := (d_{ab}+d_{bc}+d_{ca})/2$.

The pricing subproblem II is defined based on the same decision variables $\boldsymbol{x}$ and r of pricing subproblem I, but without $c^{\hat{x}}$ and $c^{\hat{y}}$.

[Pricing subproblem II]

$$\min \quad (11)$$

$$\text{s.t.} \quad r \geq R_{i_1 i_2 i_3} + \tilde{M}'(x_{i_1} + x_{i_2} + x_{i_3} - 3), \qquad \forall i_1, i_2, i_3 \in N \tag{16}$$

$$r \geq d_{i_1 i_2}/2 + \tilde{M}'(x_{i_1} + x_{i_2} - 2), \qquad \forall i_1, i_2 \in N \tag{17}$$

$$(13), (14)$$

The pricing subproblem II has the same objective function as the pricing subproblem I. As mentioned above, the constraint relating to the minimum coverage radius and the set of demand points can be defined by the constraint over every two-element and three-element subset. The radius of the minimum covering circle, $R_{i_1 i_2 i_3}$, is defined for every three-element subset of I. Constraint (16) ensures that the minimum coverage radius should be the same or larger than the radius of the minimum covering circle of any three demand points chosen in the solution of the subproblem. Constraint (17) relates the minimum

coverage radius to the radius of the minimum covering circle defined by two demand points.

In a departure from the quadratic constraint model of subproblem I, subproblem II employs an array of mixed-integer linear constraints to delineate the coverage distance. This approach not only simplifies the mathematical representation but also endows the subproblem with a polyhedral feasible set, facilitating a convex LP relaxation. Such structural refinement underscores the UVCP's compatibility with the B&P algorithm and optimization solver, enhancing the model's tractability.

While Berman et al. (2009) acknowledged the theoretical challenge of identifying minimal subsets without resorting to brute force enumeration, each coverage constraint within subproblem II is precisely aligned with one minimal subset. Reflecting the assertion of Berman et al. (2009), the optimal UVCP solution can be developed as a union of the minimal subset, and each minimal subset can be defined from a solution of the pricing subproblem II.

Although the same technique can be applied to reformulate the standard problem, it is used only for the extended formulation because of two limitations. As analyzed in Park et al. (2020), the continuous relaxation neutralizes the coverage distance constraint and makes the meaningless value of the continuous relaxation bound. The only difference is that in the ES in the USCP, the objective is to minimize the number of UAVs, and the continuous relaxation bound is 1. In contrast, in the UVCP, the continuous relaxation bound equals the fixed cost, F. Another limitation is the size of the problem. Because the reformulation requires $|N|(|N|^2+5)/6 (=_{|N|} C_3 +_{|N|} C_2 +_{|N|} C_1)$ constraints to define coverage distance constraints, the size of the problem increases quickly as the number of demand points increases. For example, if $|N|$ equals 50 and 100, then 20,875 and 166,750 constraints are required, respectively. It was observed that some problems of more than 50 nodes could not even be loaded to the commercial solver. Even for problems with only ten nodes, the commercial solvers could not solve the problem within one hour because of the weak lower bounds and the symmetries of the branching tree.

5.2. Equivalence of the subproblem

The equivalence of the two subproblems is shown in this section. Although the feasible regions of the continuous relaxation of two subproblems are different, the integer decision variable bounds the feasible region, making them equivalent.

Theorem 1. *Pricing subproblems I and II are equivalent.*

Because the two problems have the same objective function, it is only necessary to show that the feasible set of both problems is the same. Let a feasible set of the pricing subproblem I be S_I and a feasible set of the pricing subproblem II be S_{II}.

Proof ($(\Rightarrow)$). We show that $S_I \subseteq S_{II}$. Let a feasible solution $\psi = (c^{\hat{x}}, c^{\hat{y}}, r, \boldsymbol{x}) \in S_I$. Using the proof of contradiction, let us assume that $\exists i_1, i_2, i_3 \in J$ such that $r, x_{i_1}, x_{i_2}, x_{i_3} \notin S_{II}$. We are focused on the case of $i_1 \neq i_2 \neq i_3$, because if there are identical points, it is self-evident that $x_{i_1}, x_{i_2}, x_{i_3} \in S_{II}$. There are two cases related to the distances between the demand points.

(Case 1) $d^2_{i_1 i_2} \geq d^2_{i_2 i_3} + d^2_{i_3 i_1}$ (Demand points are on the same straight line or form an obtuse triangle). By the assumption, the following holds:

$$r + \tilde{M}'(2 - x_{i_1} - x_{i_2}) < \frac{d_{i_1 i_2}}{2}.$$

Because $x_{i_1}, x_{i_2} \in \mathbb{B}$ and $r \geq 0$, $x_{i_1} = x_{i_2} = 1$ and $r \leq \frac{d_{i_1 i_2}}{2}$.

$d_{i_1 j} \leq r$, $d_{i_2 j} \leq r$ $(\because \psi \in S_I) \Longrightarrow d_{i_1 j} + d_{i_2 j} \leq 2r < d_{i_1 i_2}$, which is false by the triangle inequality.

(Case 2) $d^2_{i_1 i_2} < d^2_{i_2 i_3} + d^2_{i_3 i_1}$. Similar to Case 1, the following holds:

$$r + \tilde{M}'(3 - x_{i_1} - x_{i_2} - x_{i_3}) < R_{i_1 i_2 i_3} \Longrightarrow x_{i_1} = x_{i_2} = x_{i_3} = 1, r < R_{i_1 i_2 i_3}.$$

However, for i_1, i_2 satisfying $d_{i_1 j} \leq r$, $d_{i_2 j} \leq r$, $d_{i_3 j} > R_{i_1 i_2 i_3}$ holds, which proves the false assumption.

($\Leftarrow$) We show that $S_{II} \subseteq S_I$. Let a feasible solution $\nu = (r, \boldsymbol{x}) \in S_{II}$. For set of demand points that satisfies $x_i = 1$ in a solution ν, there exists a unique minimum covering circle, and the circle can be defined by at most three points in the set.

If the circle is defined by two points, i_1 and i_2, $(c^{\hat{x}}, c^{\hat{y}}, r, \boldsymbol{x})$ satisfies Constraint (12), where the position $(c^{\hat{x}}, c^{\hat{y}})$ is defined as:

$$c^{\hat{x}} = \frac{a^{\hat{x}}_{i_1} + a^{\hat{x}}_{i_2}}{2}, \quad c^{\hat{y}} = \frac{a^{\hat{y}}_{i_1} + a^{\hat{y}}_{i_2}}{2}.$$

If the circle is defined by three points, i_1, i_2, and i_3, the solution is defined as:

$$c^{\hat{x}} = \frac{((a^{\hat{x}}_{i_1})^2 + (a^{\hat{y}}_{i_1})^2)(a^{\hat{y}}_{i_2} - a^{\hat{y}}_{i_3}) + ((a^{\hat{x}}_{i_2})^2 + (a^{\hat{y}}_{i_2})^2)(a^{\hat{y}}_{i_3} - a^{\hat{y}}_{i_1}) + ((a^{\hat{x}}_{i_3})^2 + (a^{\hat{y}}_{i_3})^2)(a^{\hat{y}}_{i_1} - a^{\hat{y}}_{i_2})}{2[a^{\hat{x}}_{i_1}(a^{\hat{y}}_{i_2} - a^{\hat{y}}_{i_3}) + a^{\hat{x}}_{i_2}(a^{\hat{y}}_{i_3} - a^{\hat{y}}_{i_1}) + a^{\hat{x}}_{i_3}(a^{\hat{y}}_{i_1} - a^{\hat{y}}_{i_2})]}$$

$$c^{\hat{y}} = \frac{((a^{\hat{x}}_{i_1})^2 + (a^{\hat{y}}_{i_1})^2)(a^{\hat{x}}_{i_3} - a^{\hat{x}}_{i_2}) + ((a^{\hat{x}}_{i_2})^2 + (a^{\hat{y}}_{i_2})^2)(a^{\hat{x}}_{i_1} - a^{\hat{x}}_{i_3}) + ((a^{\hat{x}}_{i_3})^2 + (a^{\hat{y}}_{i_3})^2)(a^{\hat{x}}_{i_2} - a^{\hat{x}}_{i_1})}{2[a^{\hat{x}}_{i_1}(a^{\hat{y}}_{i_2} - a^{\hat{y}}_{i_3}) + a^{\hat{x}}_{i_2}(a^{\hat{y}}_{i_3} - a^{\hat{y}}_{i_1}) + a^{\hat{x}}_{i_3}(a^{\hat{y}}_{i_1} - a^{\hat{y}}_{i_2})]}.$$

Both $S_I \subseteq S_{II}$ and $S_{II} \subseteq S_I$ are shown and proves the claim. □

One can solve the CG of the UVCP with the pricing subproblem II by Theorem 1.

6. Fixed-radius heuristic

The pricing subproblem II has an LP relaxation with a convex feasible set. Also, the subproblem consists of linear constraints so that the commercial solver can handle the problem in a more numerically stable procedure. However, as mentioned above, the pricing subproblem II required $|N|(|N|^2+5)/6$ constraints to model the coverage distance constraint for N demand points. The size of constraints can rapidly increase in the case of a large number of demand points. On the other hand, the pricing subproblem I required one constraint per one demand point, so the size of the subproblem does not drastically increase uncontrollably, while it is not solvable by itself.

We developed a heuristic to harness the findings of the USCP that the B&P algorithm could provide to the solution of the large-sized problem in a short computation time. To harness the efficiency of the B&P algorithm observed in the USCP, the fixed-radius heuristic (FRH) tactically approximates the original pricing subproblem I by discretizing and fixing the coverage radius. This approach aligns the feasible set of the FRH with that of the USCP, enabling the heuristic to explore various fixed radii in discrete steps and select the radius yielding the most advantageous (most negative) reduced cost for the new column.

To put it succinctly, the FRH solve the approximation of the original pricing subproblem I by the decomposition over the various radii, r. The continuous relaxation of each decomposed problem has the convex feasible set, and can be solved by the optimization efficiently. The mathematical formulation of the decomposed problem of radius, R, is provided as follows:

$$\min \quad (11)$$

$$\text{s.t.} \quad (a^{\hat{x}}_i - c^{\hat{x}})^2 + (a^{\hat{y}}_i - c^{\hat{y}})^2 \leq R^2 + \tilde{M}(1 - x_i), \qquad \forall i \in N \qquad (18)$$

$$x_i \in \mathbb{B}, \qquad \forall i \in N \qquad (19)$$

$$c^{\hat{x}}, c^{\hat{y}} \in \mathbb{R}, \qquad (20)$$

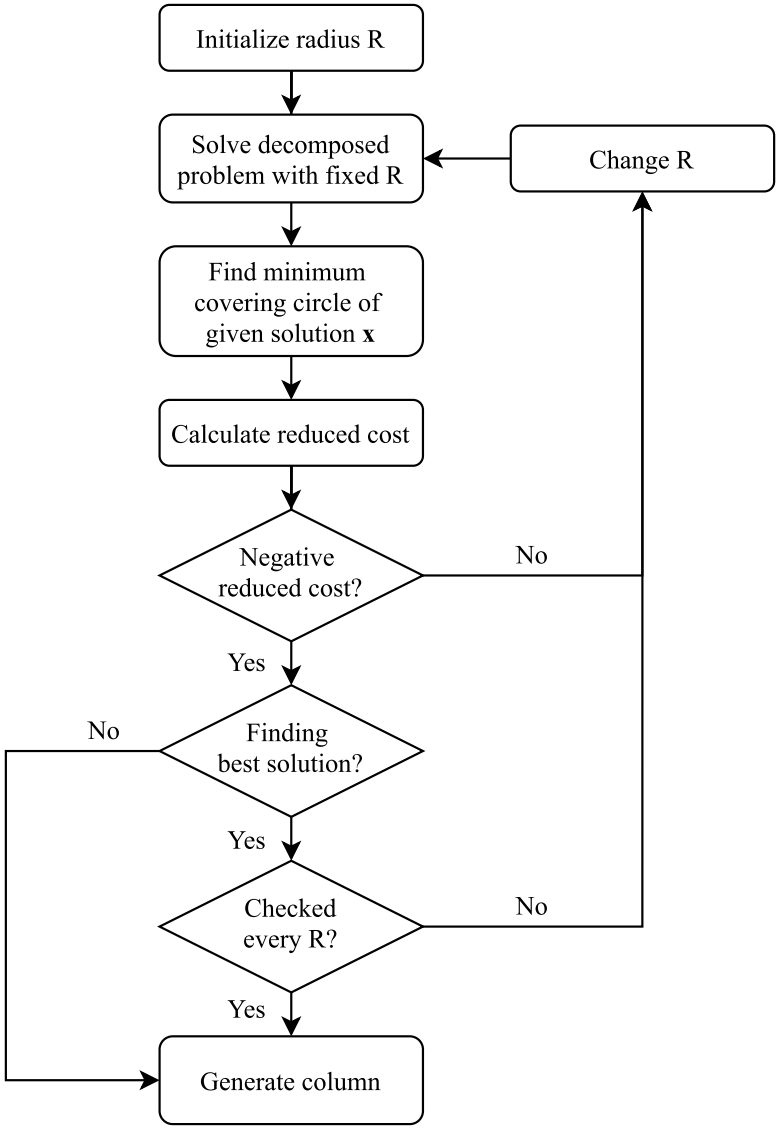

Fig. 2. The procedure of the fixed-radius heuristic.

Upon determining a solution set $\bar{N}$ of demand points for a given radius, R, the actual radius, r, used for calculating reduced costs and generating columns, is derived from the minimum covering circle of $\bar{N}$, potentially smaller than the initially fixed radius. This adjustment ensures the solution's feasibility and optimality within the heuristic's framework. Welzl's algorithm (Welzl, 1991) or a modified optimization formulation related to the continuous single facility location problem may be employed to ascertain this minimum covering circle:

$$\min \quad r \tag{21}$$

$$\text{s.t.} \quad (a_i^{\hat{x}} - c^{\hat{x}})^2 + (a_i^{\hat{y}} - c^{\hat{y}})^2 \le r^2, \qquad \forall i \in \bar{N} \tag{22}$$

(14), (15)

Because the original problem of the FRH, pricing subproblem I, has the nonconvex feasible set, the FRH or the hybrid algorithm of the FRH and Newton's method cannot find every optimal solution of the original problem. However, as mentioned above, the actual radius, r, is changed to be local optimal after fixing the demand points to be covered, so it is tentatively expected that the heuristic can work as a sieve under the appropriate decomposition interval that can find the most of the effective solutions. In one iteration of the CG, the FRH can stop when a solution with the negative reduced cost is found or can check every possible radius, R, and generate a column with the most negative reduced cost. The procedure of the FRH is presented in Fig. 2 (below).

Incorporating the FRH into a hybrid algorithm further enhances the CG process's efficiency, especially for large-scale problems. Initially, the FRH swiftly generates promising columns, transitioning to the more computationally demanding pricing subproblem II when diminishing returns from the heuristic necessitate a precise convergence toward optimality.

The effectiveness of the FRH and its hybrid implementation are empirically validated through computational experiments detailed in Section 7. These analyses underscore the heuristic's capability to streamline the solution process for the UVCP, demonstrating its value as a tool for enhancing the practical applicability of the B&P algorithm in complex UAV deployment scenarios.

7. Computational experiments

The computational experiments were conducted to compare the performances of the proposed solution algorithms to the benchmark genetic algorithm proposed in Berman et al. (2009). The dataset used in the computational experiment is introduced in Section 7.1. The B&P

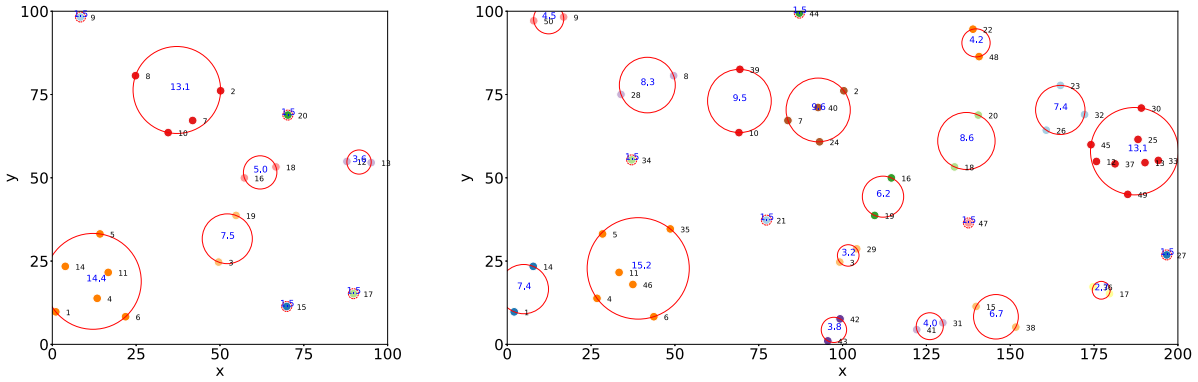

(a) B&P sol. of $1 \times 1, |N| = 20$ (b) B&P sol. of $2 \times 1, |N| = 50$

Fig. 3. Example of the solution for small-sized problem.

algorithm and the FRH were developed in FICO Xpress 8.5 and solved with Xpress-Optimizer 33.01.02. Because the coverage distance-related cost function was modeled as a quadratic function, the pricing subproblem II was solved by the Xpress MIQP solver. The FRH was operated in an Xpress MIQCQP solver using the barrier method. The genetic algorithm was developed and solved in Python 3.6. Experiments were performed with an AMD Ryzen^{TM} 7 2700X 8-Core CPU at 3.70 GHz and 32 GB of RAM running on a Windows 10 64-bit operating system.

7.1. Datasets used in the experiments

In the experiment, the fixed cost of a UAV, F, is set to be 100, and the variable operation cost function is set to be $\phi(r) = r^2$, consistent with Berman et al. (2009). We generated two distinct problem sets with uniformly distributed demand points across a 100×100 square and a 200×100 rectangle. Demand points varied across four magnitudes: 10, 20, 50, and 100, culminating in eight unique problem classes with ten instances each. This design choice, although more conservative than the larger datasets used in Berman et al. (2009), was dictated by the unrealistic optimal solutions observed in their work and by our own preliminary tests, underscoring the necessity for a more restrained problem scale to ensure realism and tractability.

The problem of Berman et al. (2009) is that the research compares the performances of the heuristics, so it does not have decent benchmark solutions. For example, Berman et al. (2009) reported that the GA could find the best-known solutions even for the large-sized problem classes, including 5000 and 10,000 demand points. However, the proposed solutions have one UAV being operated, and every demand point is covered by the UAV, which is unrealistic. Even in the smallest problems, we found that the GA proposed by Berman et al. (2009) could not find optimal solutions. Figs. 3 and 4 (below) show the example solutions of the UVCP. The demand points are indexed and placed on the xy-plane. Each empty circle covering the demand points represents a UAV and the covering circle. For example, in Fig. 3(a), demand points 2, 7, 8, and 10 are covered by a single UAV with a coverage radius = 13.1. For ease of understanding, the UAVs that cover single demand points are drawn with dotted covering circles with a coverage radius of 1.5, which is chosen arbitrarily for figures.

7.2. Solution algorithms

In the computational experiments, the GA proposed in Berman et al. (2009) is used as a benchmark. To minimize the information held on each chromosome, the chromosome only consists of the position of the UAV and does not contain information of the allocation decision. The GA consists of three parts—local optimization, neighborhood search, and mating and evaluation. The local optimization part deletes the UAV that might not be used and relocates the UAVs to the local-optimal positions. Based on the current positions of the UAVs, each demand point is allocated to the closest UAV, and the UAVs without any demand point are removed. The remaining UAVs are relocated by solving the continuous single facility location problem. The procedure iterates until there are no more UAVs changing their locations. The local optimization is incorporated when a new individual is generated, including within the initial population, within the neighborhood search, and within the mating and producing of offspring. The neighborhood search part also finds a possible removal of a UAV that improves the objective function. By randomly removing one UAV, we can test the improvement of the objective function. The mating for a new offspring is done by merging two individuals and the repetition of the neighborhood search to the local optimum.

The B&P algorithm, the FRH, and the hybrid algorithm using FRH in the B&P algorithm (FRH-B&P) are compared in the experiment. The B&P and the FRH-B&P are the exact algorithms, and the FRH is an approximation algorithm.

We used the hybrid approach for the B&P algorithm itself to speed up the CG procedure. If the maximum coverage distance was limited, the feasible region of the subproblem II decreased, and so did the computation time. Also, when the CG was solved to the optimal, the solution tended to have only a limited number of UAVs covering too large an area. In the early stage, the coverage distance was limited to the realistic size in the subproblem II. We denoted this as a limited-coverage subproblem. The limited-coverage subproblem contained an additional constraint, $r \leq R_{lim}$. When the limited-coverage subproblem could not find a solution with a negative reduced cost, the subproblem II without the limit of the coverage distance was used in the CG. For convenience, we denote the original subproblem II as a full-coverage subproblem in this section.

Because the limited-coverage subproblem provided the lower bound in the CG, if the lower bound and the primal bound satisfied the termination condition, the CG of the node could be terminated without solving the full-coverage subproblem. In the experiment, there were many instances in which the CG with the limited-coverage subproblem generated most of the columns required. In those cases, after the switch to the full-coverage subproblem, the full-coverage problem could not find the improving columns, or the CG was finished after a few iterations. This tendency and the proper value of the R_{lim} might be changed when a different objective function is employed. The CG algorithm of the hybrid approach is presented in Fig. 5 (below). Note that the CG of the FRH-B&P shares a similar structure if the FRH replaces the limited-coverage subproblem.

In the problems of $|N| = 50$ and 100, we generated the initial columns based on the solution of the GA. An individual of the GA could be translated to several columns by allocating each demand point to

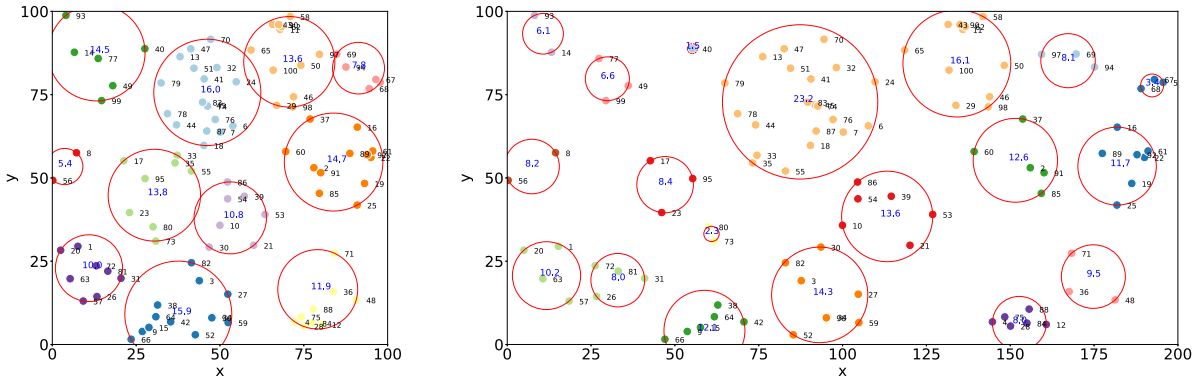

(a) FRH-B&P sol. of $1 \times 1, |N| = 100$.

(b) FRH-B&P sol. of $2 \times 1, |N| = 100$.

Fig. 4. Example of the solution for large-sized problem.

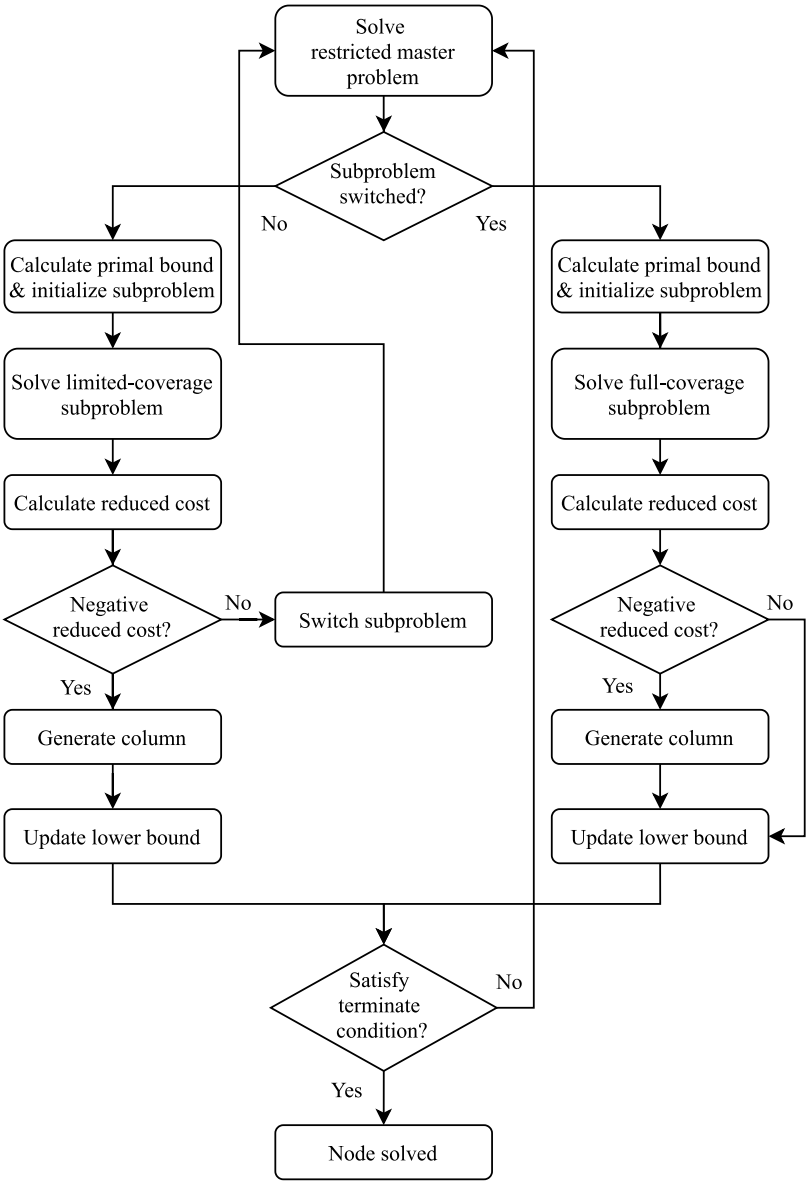

Fig. 5. The procedure of the column generation algorithm with a hybrid approach.

Table 2
Results related to the computation speed.

Dim	$\|N\|$	*#solved*				*Time(s)*				$Gap_L(\%)$		
		B&P	FRH	FRH-B&P	GA	B&P	FRH	FRH-B&P	GA	B&P	FRH	FRH-B&P
1 × 1	10	10	10	10	10	0.12	0.55	0.68	70.04	0.0	0.0	0.0
	20	10	10	10	10	1.14	7.02	8.38	517.44	0.0	0.0	0.0
	50	10	10	9	9	754.69	308.31	1105.51*	2679.13*	0.0	0.0	< 0.05
	100	0	8	0	0	3600*	2337.18*	3600*	3600*	213.5	0.1	114.1
2 × 1	10	10	10	10	10	0.08	0.43	0.52	56.21	0.0	0.0	0.0
	20	10	10	10	10	0.63	2.16	2.85	367.43	0.0	0.0	0.0
	50	10	10	10	8	84.43	162.73	229.85	1933.28	0.0	0.0	0.0
	100	0	8	0	0	3600*	1623.80	3600*	3600*	79.5	0.0	7.4

* There are instances not solved within the time limit.

Table 3
Results related to the optimality (objective value)

Dim	$\|N\|$	*#Opt/#Best*				*Objective value*				*Gap(%)*			
		B&P	FRH	FRH-B&P	GA	B&P	FRH	FRH-B&P	GA	B&P	FRH	FRH-B&P	GA
1 × 1	10	10/10	5/5	10/10	10/10	823.2	862.7	823.2	823.2	0.0	5.4	0.0	0.0
	20	10/10	3/3	10/10	9/9	1375.1	1486.4	1375.1	1375.8	0.0	8.4	0.0	0.1
	50	10/10	4/4	10/10	2/2	2312.1	2321.8	2312.1	2332.4	0.0	0.4	0.0	0.9
	100	0/0	0/7	0/9	0/2	3645.2	3059.9	3035.4	3092.0	19.3	0.1	< 0.05	7.4
2 × 1	10	10/10	9/9	10/10	10/10	911.2	916.0	911.2	911.2	0.0	0.6	0.0	0.0
	20	10/10	5/5	10/10	10/10	1668.7	1696.2	1668.7	1668.7	0.0	1.7	0.0	0.0
	50	10/10	10/10	10/10	7/7	3084.8	3084.8	3084.8	3095.5	0.0	0.0	0.0	0.4
	100	0/0	0/3	0/9	0/2	4590.5	4419.8	4064.4	4436.1	4.5	0.7	< 0.05	1.1

Table 4
Results related to the optimality (# of UAVs)

Dim	$\|N\|$	#UAV			
		B&P	FRH	FRH-B&P	GA
1 × 1	10	7.0	7.0	7.0	7.0
	20	9.5	8.6	9.5	9.5
	50	11.8	12.2	11.8	12.9
	100	15.4	12.7	12.8	12.5
2 × 1	10	8.3	8.2	8.3	8.3
	20	13.5	13.3	13.5	13.7
	50	20.4	20.4	20.4	20.2
	100	23.8	22.6	22.9	23.7

the nearest UAV. After 200 generations or 200 s of the GA, 20 best individuals were generated as the initial columns and were included in the FRH and the FRH-B&P for the fast convergence.

Furthermore, the restricted master heuristic (RMH) was used for the large-sized problems that could not find the optimal solution within the time limitation. The RMH is one of the most widely used heuristics related to the B&P algorithm. Based on the current variables (columns), one could solve the problem with the extended formulation using the MILP solvers. This algorithm is also called the *price-and-branch*, especially when it is executed after the termination of the root node CG, because the columns are generated first, and the branching takes place later. The UVCP does not consider the capacity constraint and assumes homogeneous UAVs. Thus, the RMH solved a small-sized, basic set partition problem and did not require a computation time longer than 0.01 s, even for the largest problems we experimented with.

7.3. Algorithmic performances

We compared the performances of the B&P, the FRH, and the FRH-B&P. The GA proposed by Berman et al. (2009) is used for the benchmark. The limitation of maximum computation time was set to 3600 s.

First, the algorithmic performances were compared based on the computation speed and the optimality. Second, a further analysis of the performances of the CG and the B&P was conducted. Third, the performance of the additional techniques, including the initial columns and the limited-coverage subproblem, were analyzed.

For the first analysis, the computation speed of the B&P algorithm, the FRH, and the hybrid FRH-B&P algorithm were compared against each other and also compared against the benchmark GA. For the instances solved within the time limitation, the computation time was recorded, and for the unfinished instances, the final gap between the primal bound and the best lower bound was compared, in order to measure the convergence of the algorithm. The optimality of the results could be resolved in two ways. First, for the problems solved to the optimal, the limitation of the approximation algorithm, FRH, could be shown. For the unfinished problems, the feasible solutions and the primal bounds found by each algorithm could be compared. For each algorithm, the number of instances that were solved to the optimal were counted. The algorithms that could be found to be the best feasible solution for the unsolved instances were identified, and the optimality gap was compared. Also, the number of UAVs operated in the best feasible solution was compared.

In Tables 2–4 (below), the results are summarized by the average of 10 instances of each problem class. The columns in these tables are defined as follows:

- *Dim*: the dimension of the xy-plane. 1 × 1 and 2 × 1 represent 100 × 100 and 200 × 100 planes, respectively.
- $|N|$: the number of demand points.
- *#solved*: the number of the solved instances, not necessarily to the optimal.
- *Time*: the average of the computation time. For the problems not solved within the time limitation, the time limit was used to calculate the average, and was marked with an asterisk (*).
- Gap_L: the average of the gap between the primal bound (the best feasible solution: BFS) and the best lower bound (BB). Gap_L was used to evaluate the algorithm's convergence speed for the instances not solved within the time limit.

$$Gap_L = \frac{(\text{BFS}) - (\text{BB})}{(\text{BFS})} \times 100\%$$

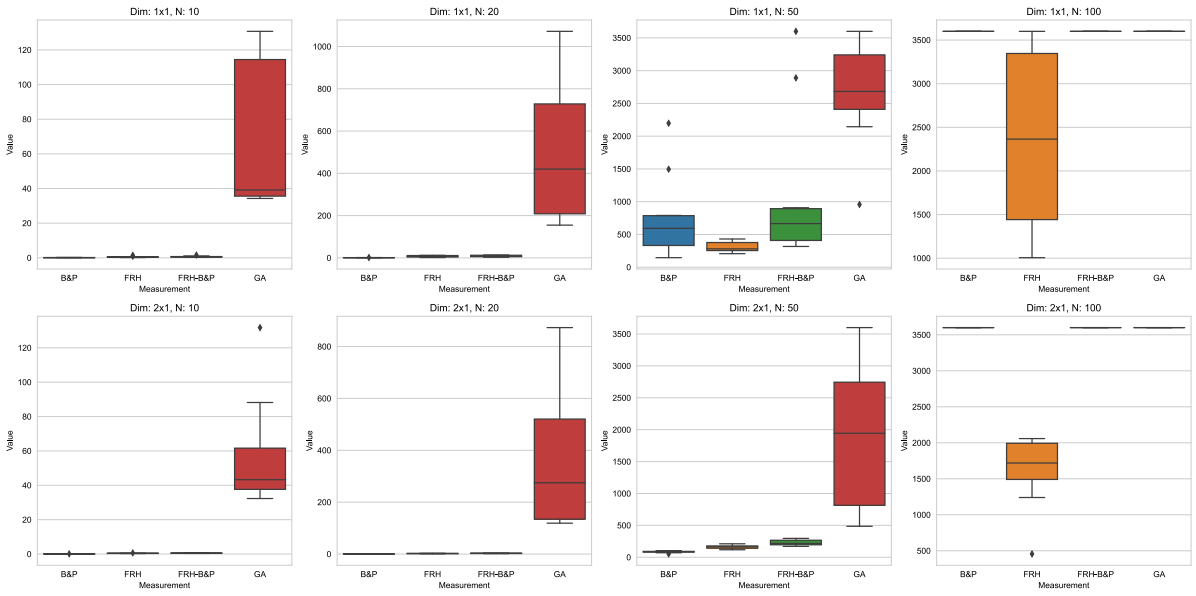

Fig. 6. The computation speed of solution algorithms.

Table 5
Results related to the CG & branching.

Dim	$\|N\|$	*#Nodes*	*#Iter*			*#Columns*		
		FRH	B&P	FRH	FRH-B&P	B&P	FRH	FRH-B&P
1 × 1	10	1.0	5.2	4.5	9.9	13.3	13.9	17.3
	20	1.0	15.5	17.2	32.1	33.5	37.1	50.0
	50	1.0	131.2	77.1	125.1*	179.2	154.9	201.4*
	100	1.1*	192.2*	572.7*	631.8*	292.2*	733.6*	765.8*
2 × 1	10	1.0	3.7	2.9	6.8	11.7	12.0	13.9
	20	1.0	9.1	8.9	18.0	27.1	28.4	35.5
	50	1.0	50.4	27.8	50.7	98.4	104.0	124.9
	100	2.3	160.0*	204.8	256.6*	260.0*	380.3	432.1*

* There are instances not solved within the time limit.

- *#Opt*: the number of instances for which the algorithm provided the optimal solution.
- *#Best*: the number of instances for which the algorithm provided the BFS, including the optimal solution.
- *Gap*: the average of the gap between the objective value of the BFS among every algorithm and the current algorithm.

$$Gap = \frac{(\text{obj. value of an algorithm}) - (\text{obj. value of the BFS})}{(\text{obj. value of the BFS})} \times 100\%$$

- *#UAV*: the average of the number of UAVs operated in the BFS.

The rapidly changing environment of UAV operation demands fast decisions. Table 2 and Fig. 6 show that the proposed algorithms outperform the benchmark GA from the standpoint of computation speed. For the smallest problems of $|N| = 10$ and 20, the B&P algorithm without any heuristic and GA initial columns could solve the problem with the fastest computation time among the algorithms while providing the optimal solution. The B&P solved 33 out of 40 of the smallest problems within one second, which enabled the algorithm to be used for rapidly changing situations. Every solution algorithm could solve most of the small-sized instances with fewer than 50 demand points. Even though the possible number of the minimal subset had the dimension of $|N|^3$, and Berman et al. (2009) anticipated that the exponential number of the power set had to be checked, in the optimal solution, only a limited number of the columns were used. Because of the strong LP bound of the extended formulation of the B&P algorithm, the CG required only a minimum number of iterations to find the optimal solution. One of the essential characteristics of the UVCP is that the CG provided the integer solutions. That means that the branching is not required while solving the problem, a point that will be introduced in the second analysis, with Table 5 (below).

Because the FRH and the FRH-B&P algorithms are proposed for large-sized problems, we focused on the problem class of $|N| = 100$ when comparing the performances of those algorithms. Even though the exact algorithms, the B&P and the FRH-B&P, could not solve the large-sized problems within the time limits, the FRH could solve the eight instances within the time limits. In Table 3, it can be observed that the FRH could find the best feasible solution from 10 out of 20 instances and that the FRH-B&P algorithm could find the BFS from 18 instances. Furthermore, the *gap* between the BFS and the FRH was less than one percent, which shows the effectiveness of the initial columns and the FRH as heuristics to provide a feasible solution. Still, to ensure or measure the optimality, the following B&P algorithm was required. Moreover, there are instances in which the FRH-B&P converged almost to the optimal. For example, in four instances of the 2 × 1 dimension, the Gap_L were lower than 0.001 percent. The *Gap* between the optimal solution and the solution of the FRH decreased as the size of the problem increased. This meant that the limitation of the approximation algorithm could be diluted when solving a large-sized problem.

Even though the GA could find the optimal solutions for some small-sized problems, it required a longer computation time for the convergence. The GA might have found the optimal solution earlier than the finished time reported in Table 2. However, because the GA did not have a lower bound to measure the true convergence of the solution algorithm, it required additional computation to distinguish

the termination. Thus, it was observed that in the small-sized problems, the B&P algorithm without any initial columns and heuristics could be the best choice that could solve the optimal solution in a short computation time. For the large-sized problems of $|N| = 100$, the FRH-B&P algorithm with the GA initial columns could be the best choice. If the computation time provided a hard limitation while solving the large-sized problem, the FRH with the GA initial columns could provide time-efficient solutions.

Observations from Park et al. (2020) regarding the B&P's enhanced performance with *sparse* problem configurations were corroborated, with the 2×1 dimension problems facilitating swifter algorithmic convergence. This dimensional influence is substantiated by the comparative analysis of computation times across different problem scales (refer to Table 2).

Analysis of UAV utilization across algorithms (Table 4) did not reveal a direct correlation between the number of deployed UAVs and the optimality gap. However, instances of non-converged CG processes within the B&P algorithm frequently resulted in solutions deploying an excessive number of UAVs, highlighting a critical consideration for operational efficiency and cost-effectiveness in UAV system deployment. This study's findings provide a foundation for further research into the operational dynamics of UAV systems, particularly in relation to cost structures and the impact of spatial distribution on algorithmic efficiency. A nuanced understanding of UAV deployment strategies, informed by comprehensive cost analyses and operational objectives, will be crucial for the practical implementation of UAV systems in real-world scenarios.

For the second analysis, the number of iterations and the number of generated columns were compared through the B&P and the heuristic-related algorithms. The branching and the nodes in the branching tree were also analyzed. In the B&P algorithms, the basic initial columns were generated, where one UAV covered one demand point. Thus, the cost of the basic initial column only consisted of the fixed cost of a UAV, 100. The FRH-B&P algorithm started with the FRP. After the FRP was finished, the full B&P algorithm was started, based on the columns generated in the FRP. The number of iterations and the columns of the FRP-B&P were the summation of the one executed in the FRP and the following B&P. The columns in Table 5 are defined as follows:

- $\#Nodes$: the average number of the nodes generated in the branching trees. For the problems not solved within the time limitation, the current value was used to calculate the average, and was marked with an asterisk (*).
- $\#Iter$: the average number of the iterations executed in the CG and the B&P algorithm.
- $\#Columns$: the average number of the columns generated in the CG and the B&P algorithm.

In the experiment, it was observed that for the exact algorithms of the B&P and the FRH-B&P, the root node CG provided the optimal integer solution. Thus, without any corresponding branching, the optimization algorithm was terminated. In Table 5, only the FRH had the column of the average number of nodes generated in the branching trees. Furthermore, even the FRH had the small value of $\#Nodes$. Compared to the results in the USCP, this identified one of the most important characteristics of the UVCP.

The difference of the nodes between the UVCP and the USCP did not originate from the structure of the objective function, which shows that the branching still happened in the FRH. Also, unlike in the USCP, the columns provided by the FRH were still "tight". Therefore, it is difficult to say that the columns that are not tight caused the difference.

The only possibility left is that the subproblem of the UVCP solved the CG to the optimal without any restriction of the coverage distance. As mentioned in Berman et al. (2009), there exists an optimal solution of the UVCP that is a union of the minimal subsets. Because each minimal subset corresponds to a column in the extended formulation, there exists an optimal solution of the UVCP that is a union of the columns. Our conjecture is that in the UVCP, both the fractional solution and the negative reduced cost are related, and if the restricted master problem has every column used in the optimal solution of the UVCP, then the subproblem does not have a new column with a negative reduced cost. Also, every minimal subset is feasible in the subproblem, so the root node CG will be able to find every minimal subset required in the optimal solution of the UVCP. This characteristic of the UVCP highlights the advantages of the speed-up techniques of the CG.

Table 6
Results related to the lower bounds.

Dim	$\|N\|$	*Lower bounds*			$Gap_L(\%)$
		B&P	B&P w. clm.	FRH-B&P	B&P w. clm.
1×1	10	823.2	823.2	823.2	0.0
	20	1375.1	1375.1	1375.1	0.0
	50	2312.1	2304.0	2312.1	0.4
	100	−4142.9	−623.4	−407.2	120.5
2×1	10	911.2	911.2	911.2	0.0
	20	1668.7	1668.7	1668.7	0.0
	50	3084.8	3084.8	3084.8	0.0
	100	912.8	3760.5	4064.4	14.3

As mentioned above, the FRH-B&P solved the original B&P algorithm after finishing the FRH. Therefore, in the FRH-B&P, the iterations already executed in the FRH were added when calculating its number of iterations. In the problem class of $|N| = 50$, the number of generated columns in the FRH-B&P was larger than the number generated in the B&P algorithm, even though the FRP-B&P required fewer numbers of iterations. This was originated by the GA initial columns, which were generated before the FRH. The FRH, admittedly, can provide efficient columns rapidly; those columns are not the columns with the most negative reduced cost, which are solved in the original pricing subproblem. Thus, the number of columns generated in the FRH and the FRH-B&P tended to be larger than in the B&P.

As mentioned above, it was easier to solve the sparse problems, so the problems with the 2×1 dimension required fewer iterations than the problems with the 1×1 dimension, and required fewer columns. Note that the B&P algorithm required only a minimum number of columns while solving the problems to the optimal. Compared to the total number of the minimal subset, which had the dimension of $|N|^3$, the number of the iterations and the columns stayed less than 1000, even for the largest problems. Thus, when the RMH was used for the largest problems that were not solved within the time limit, the computation time of the RMH stayed less than 0.01 s for every problem.

For the third analysis, additional techniques to speed up the computation were analyzed. As mentioned in Section 7.2, the FRH and the FRH-B&P started with the initial columns generated by the GA for the problems of $|N| = 50$ and 100. Although the GA required a long computation time to find good individuals, the embedded heuristic inside the GA could help find the local optimal subset of demand points. A solution of the GA was decoded into the mathematical model and divided into multiple columns to be included in the solution algorithms. In the analysis, the B&P with the GA initial columns was also tested to see the improvement of the lower bound.

Also, the effect of the limitation of the coverage was analyzed. In the hybrid algorithm of the limited and full-coverage subproblems, the time spent for each subproblem, along with the number of iterations, was compared. The columns in Tables 6 and 7 (below) are defined as follows:

- B&P w. clm.: the B&P algorithm starting with initial columns generated by the GA.

Table 7
Comparison of the hybrid algorithm and initial column.

Dim	$\|N\|$	B&P			B&P w. clm.			B&P		B&P w. clm.	
		$Time_{lim}$	*Time*	*Ratio*	$Time_{lim}$	*Time*	*Ratio*	$\#Iter_{lim}$	*#Iter*	$\#Iter_{lim}$	*#Iter*
1 × 1	10	0.09	0.12	75.1	31.98	32.02	99.9	4.2	5.2	1.9	3.0
	20	0.93	1.14	81.1	127.11	127.35	99.8	14.5	15.5	6.7	7.8
	50	160.54	754.69	34.7	275.72	924.41*	54.3*	122.5	131.2	68.1	73.1*
	100	3600*	3600*	100*	3600*	3600*	100*	192.2*	192.2*	183.2*	183.2*
2 × 1	10	0.04	0.08	51.1	20.98	21.01	99.8	2.7	3.7	1.2	2.2
	20	0.41	0.63	63.5	63.42	63.65	99.5	8.1	9.1	2.7	3.7
	50	54.79	84.43	66.1	139.55	170.58	82.3	49.2	50.4	24.4	25.5
	100	3600*	3600*	100*	3600*	3600*	100*	160.0*	160.0*	123.8*	123.8*

* There are instances that the limited-coverage subproblem is not finished within the time limit.

- $Time_{lim}$: the average of the computation time spent on the limited-coverage subproblem. For the problem class in which the limited-coverage subproblem was not finished within the time limitation, the time limit was used to calculate the average, and was marked with an asterisk (*).
- $\#Iter_{lim}$: the average of the number of iterations executed in the limited-coverage subproblem.

By generating multiple initial columns with the GA, the B&P could improve both primal and lower bounds when solving the large-sized problems. The effective initial column decreased the number of iterations required for the column generation. However, for the small-sized problems, the advantages did not show up because the B&P algorithm without initial columns did not require a large number of iterations by itself. In Table 7, the difference between the number of iterations was not significant in the problem class of $|N| = 10$ and 20. The effective GA initial columns contained the columns covering a larger distance than the limit set in the limited-coverage subproblem. In the B&P algorithm using a hybrid approach without initial columns, when the size of the problem exceeded a certain level, it became harder to solve the last few iterations of the full-coverage subproblem. This originated from two reasons. First, the full-coverage subproblem took a longer computation time than the limited-coverage subproblem. Second, it became more challenging to solve the subproblem when the CG algorithm converged. Thus, in the problem class of $|N| = 50$, the ratio between $time_{lim}$ and $time$ stayed very low. Especially in the instances with the dimension of 2×1, it took an extra 30 s to execute one iteration of the full-coverage subproblem. However, the B&P with GA initial columns started with columns of a large coverage distance. Thus, the ratio of the computation time of the two subproblems stayed very high, meaning that there was less effort required for handling the full-coverage subproblems.

In the problem class of $|N| = 100$, both B&P and B&P with GA initial columns could not solve the problem to the optimal. Therefore, the performances were compared based on the lower bound and the Gap_L. The advantages of the FRH have already been mentioned in the previous analysis. However, some of the advantages originated from the usage of the GA initial columns. The improvement of the lower bounds by each technique was observed, and the FRH-B&P, which used both techniques, performed the best.

The advantage of the hybrid approach of the limited-coverage and full-coverage subproblems was shown in the comparison of the number of iterations. In most of the iterations in the CG, only columns with the limited coverage radius were produced. Because the full-coverage subproblem took a longer computation time while providing the same solution, it was more useful to focus on the smaller feasible region.

8. Conclusions

This paper introduced the problem of developing a flight plan of a UAV while taking into account the variable coverage area. The problem was modeled from existing literature that focused on the planar version of the variable radius covering problem by Berman et al. (2009).

The UVCP was modeled as a set covering problem without a limitation of the predefined candidate position and with an extra decision of the variable coverage distance. Although Berman et al. (2009) could not find an explicit expression of the UVCP and claimed that the UVCP is not suitable for a mathematical optimization approach, we formulated the UVCP as a mixed-integer quadratically constrained quadratic programming problem, based on the approaches proposed in Park et al. (2020). Due to the nonconvex feasible set of the continuous relaxation, the problem was not solvable by the optimization software. An extended formulation and a corresponding B&P algorithm were proposed to utilize the concept of the minimal subset. By leveraging the concept of minimal subsets and employing the minimum covering circle principle, we successfully transformed the UVCP subproblem into a tractable mixed-integer linear quadratic programming model, establishing the equivalence between this and the original formulation. The fixed-radius heuristic solved multiple fixed-radius problems of the UVCP, which had the same feasible set of the USCP (Park et al., 2020). A hybrid approach using FRH and the original B&P was developed to accelerate the computation speed of the large-sized instances. The computational results showed that the proposed B&P algorithms outperformed the benchmark GA proposed by Berman et al. (2009) whenever they could find the optimal solution with the shorter computation time for the small-sized problems. The proposed B&P algorithms had better primal bounds for the large-sized problems and could measure the convergence of the optimization by the gap between the primal and the lower bounds. One characteristic observed in the computational experiment was that the root node column generation of the B&P algorithm provided an integer solution, so that the branching was not required in the UVCP. This phenomenon underscores the critical importance of rapid CG convergence, achievable through the strategic employment of initial columns, heuristic integration, and the nuanced application of hybrid algorithmic approaches.

CRediT authorship contribution statement

Youngsoo Park: Writing – review & editing, Writing – original draft, Methodology, Formal analysis, Data curation, Conceptualization. **Chang Seong Ko:** Supervision, Conceptualization. **Ilkyeong Moon:** Writing – review & editing, Supervision, Methodology, Funding acquisition, Formal analysis, Conceptualization.

Data availability

Data will be made available on request.

Acknowledgments

The authors are grateful for the valuable comments from the area editor and three anonymous reviewers. This work was supported by the National Research Foundation of Korea (NRF) grants funded by the Korea government (Ministry of Science and ICT) (No. RS-2023-00218913 and No. RS-2024-00337285)

References

Abeywickrama, H.V., Jayawickrama, B.A., He, Y., Dutkiewicz, E., 2018. Empirical power consumption model for UAVs. In: 2018 IEEE 88th Vehicular Technology Conference. VTC-Fall, pp. 1–5. http://dx.doi.org/10.1109/VTCFall.2018.8690666.

Ahmadi-Javid, A., Seyedi, P., Syam, S.S., 2017. A survey of healthcare facility location. Comput. Oper. Res. 79, 223–263. http://dx.doi.org/10.1016/J.COR.2016.05.018.

Bélanger, V., Ruiz, A., Soriano, P., 2019. Recent optimization models and trends in location, relocation, and dispatching of emergency medical vehicles. European J. Oper. Res. 272 (1), 1–23. http://dx.doi.org/10.1016/J.EJOR.2018.02.055.

Berman, O., Drezner, Z., Krass, D., Wesolowsky, G.O., 2009. The variable radius covering problem. European J. Oper. Res. 196 (2), 516–525. http://dx.doi.org/10.1016/j.ejor.2008.03.046.

Blanco, V., Gázquez, R., da Gama, F.S., 2023. Multi-type maximal covering location problems: Hybridizing discrete and continuous problems. European J. Oper. Res. 307 (3), 1040–1054. http://dx.doi.org/10.1016/j.ejor.2022.10.037.

Capoyleas, V., Rote, G., Woeginger, G., 1991. Geometric clusterings. J. Algorithms 12 (2), 341–356. http://dx.doi.org/10.1016/0196-6774(91)90007-L.

Choi, I.-C., Chaudhry, S.S., 1993. The p-median problem with maximum distance constraints: A direct approach. Locat. Sci. 1 (3), 235–243.

Comley, W.J., 1995. The location of ambivalent facilities: Use of a quadratic zero-one programming algorithm. Appl. Math. Model. 19 (1), 26–29.

Daskin, M.S., 1983. A maximum expected covering location model: Formulation, properties and heuristic solution. Transp. Sci. 17 (1), 48–70. http://dx.doi.org/10.1287/trsc.17.1.48.

Daskin, M.S., Maass, K.L., 2015. The p-median problem. In: Laporte, G., Nickel, S., Saldanha da Gama, F. (Eds.), Location Science. Springer, pp. 21–45. http://dx.doi.org/10.1007/978-3-319-13111-5_2.

Drezner, T., 1998. Location of multiple retail facilities with limited budget constraints — in continuous space. J. Retail. Consum. Serv. 5 (3), 173–184. http://dx.doi.org/10.1016/S0969-6989(98)80009-X.

Drezner, Z., Klamroth, K., Schöbel, A., O. Wesolowsky, G., 2001. The Weber problem. In: Drezner, Z., Hamacher, H.W. (Eds.), Facility Location: Applications and Theory. Springer, pp. 1–36. http://dx.doi.org/10.1007/978-3-642-56082-8_1.

Farahani, R.Z., Asgari, N., Heidari, N., Hosseininia, M., Goh, M., 2012. Covering problems in facility location: A review. Comput. Ind. Eng. 62 (1), 368–407. http://dx.doi.org/10.1016/j.cie.2011.08.020.

Fernández, J., Pelegrı'n, B., Plastria, F., Tóth, B., 2007. Solving a Huff-like competitive location and design model for profit maximization in the plane. European J. Oper. Res. 179 (3), 1274–1287. http://dx.doi.org/10.1016/j.ejor.2006.02.005.

Gendreau, M., Laporte, G., Semet, F., 1997. Solving an ambulance location model by tabu search. Locat. Sci. 5 (2), 75–88. http://dx.doi.org/10.1016/S0966-8349(97)00015-6.

Karatas, M., Eriskin, L., 2021. The minimal covering location and sizing problem in the presence of gradual cooperative coverage. European J. Oper. Res. 295 (3), 838–856. http://dx.doi.org/10.1016/j.ejor.2021.03.015.

Karatas, M., Eriskin, L., 2023. Linear and piecewise linear formulations for a hierarchical facility location and sizing problem. Omega 118, 102850. http://dx.doi.org/10.1016/j.omega.2023.102850.

Liu, R.l., Zhang, Z.j., Jiao, Y.f., Yang, C.h., Zhang, W.j., 2019. Study on flight performance of propeller-driven UAV. Int. J. Aerosp. Eng. 2019, 6282451. http://dx.doi.org/10.1155/2019/6282451.

Paredes, J.A., Saito, C., Abarca, M., Cuellar, F., 2017. Study of effects of high-altitude environments on multicopter and fixed-wing UAVs' energy consumption and flight time. In: 2017 13th IEEE Conference on Automation Science and Engineering. CASE, pp. 1645–1650. http://dx.doi.org/10.1109/COASE.2017.8256340.

Park, Y., Nielsen, P., Moon, I., 2020. Unmanned aerial vehicle set covering problem considering fixed-radius coverage constraint. Comput. Oper. Res. 119, 104936. http://dx.doi.org/10.1016/j.cor.2020.104936.

Periyasamy, S., Khara, S., Thangavelu, S., 2016. Balanced cluster head selection based on modified k-means in a distributed wireless sensor network. Int. J. Distrib. Sens. Netw. 12 (3), 1–11. http://dx.doi.org/10.1155/2016/5040475.

Plastria, F., 2001. Continuous covering location problems. In: Drezner, Z., Hamacher, H.W. (Eds.), Facility Location: Applications and Theory. pp. 37–79. http://dx.doi.org/10.1007/978-3-642-56082-8_2.

ReVelle, C., Hogan, K., 1989. The maximum availability location problem. Transp. Sci. 23 (3), 192–200.

Sun, Y., Wang, T., Wang, S., 2019. Location optimization and user association for unmanned aerial vehicles assisted mobile networks. IEEE Trans. Veh. Technol. 68 (10), 10056–10065. http://dx.doi.org/10.1109/TVT.2019.2933560.

Thibbotuwawa, A., Nielsen, P., Zbigniew, B., Bocewicz, G., 2019. Energy consumption in unmanned aerial vehicles: A review of energy consumption models and their relation to the UAV routing. In: Świątek, J., Borzemski, L., Wilimowska, Z. (Eds.), Information Systems Architecture and Technology: Proceedings of 39th International Conference on Information Systems Architecture and Technology – ISAT 2018. Springer International Publishing, Cham, pp. 173–184.

Van Wassenhove, L.N., 2006. Humanitarian aid logistics: Supply chain management in high gear. J. Oper. Res. Soc. 57 (5), 475–489. http://dx.doi.org/10.1057/palgrave.jors.2602125.

Wallop, H., 2011. Japan earthquake: How Twitter and Facebook helped. URL https://www.telegraph.co.uk/technology/twitter/8379101/Japan-earthquake-how-Twitter-and-Facebook-helped.html. (Accessed 05 June 2023).

Wang, L., Hu, B., Chen, S., 2020. Energy efficient placement of a drone base station for minimum required transmit power. IEEE Wirel. Commun. 9 (12), 2010–2014. http://dx.doi.org/10.1109/LWC.2018.2808957.

Wankmüller, C., Truden, C., Korzen, C., Hungerländer, P., Kolesnik, E., Reiner, G., 2020. Optimal allocation of defibrillator drones in mountainous regions. OR Spectr. 42 (3), 785–814. http://dx.doi.org/10.1007/s00291-020-00575-z.

Welzl, E., 1991. Smallest enclosing disks (balls and ellipsoids). In: Maurer, H. (Ed.), New Results and New Trends in Computer Science. Springer, pp. 359–370.

Zorbas, D., Di Puglia Pugliese, L., Razafindralambo, T., Guerriero, F., 2016. Optimal drone placement and cost-efficient target coverage. J. Netw. Comput. Appl. 75, 16–31. http://dx.doi.org/10.1016/J.JNCA.2016.08.009.